

# 3D-printed, directly conductive and flexible electrodes for personalized electroencephalography

This paper was downloaded from TechRxiv (<https://www.techrxiv.org>).

LICENSE

CC BY 4.0

SUBMISSION DATE / POSTED DATE

22-08-2022 / 29-08-2022

CITATION

Xing, Le; Casson, Alex (2022): 3D-printed, directly conductive and flexible electrodes for personalized electroencephalography. TechRxiv. Preprint. <https://doi.org/10.36227/techrxiv.20537190.v1>

DOI

[10.36227/techrxiv.20537190.v1](https://doi.org/10.36227/techrxiv.20537190.v1)

# 3D-printed, directly conductive and flexible electrodes for personalized electroencephalography

Le Xing<sup>a,\*</sup>, Alexander J. Casson<sup>a</sup>

<sup>a</sup>University of Manchester, Department of Electrical and Electronic Engineering, Oxford Road, Manchester, M13 9PL, United Kingdom

## ARTICLE INFO

**Keywords:**  
EEG electrodes  
3D-printing  
Brain-Computer Interfaces (BCI)  
Directly conductive  
Steady-State Visual Evoked Potentials (SSVEP)

## ABSTRACT

Electroencephalography (EEG) is a widely used non-invasive brain monitoring technique that records the electrical signals generated within the brain, with applications ranging from epilepsy to Brain-Computer Interfaces (BCI). The electrode connecting the EEG instrumentation to the user's scalp is a key part of this system which determines the overall performance. Traditionally, disc electrodes, or fingered electrodes to pass through hair, have been used, but with a very limited number of sizes and shapes available which do not reflect all users and head-hair types. Recently, 3D-printed electrodes have been proposed for allowing personalized manufacturing and more inclusive EEG. Current 3D-printed electrodes can be physically flexible for comfort, and allow recording without a conductive gel being added. However, they are formed by printing a base structure which is then coated with Silver/Silver-Chloride to make it suitable for non-invasive brain recording. This paper presents novel 3D-printed EEG electrodes with that can be made using a directly conductive flexible filament. The resulting electrodes are gel free, coating free, can be personalized, have reduced manufacturing time, and cost less compared to previous electrodes. Our electrodes are characterized in terms of contact impedance, contact noise, on-phantom signal recording, mechanical strength, and the recording of Steady-State Visual Evoked Potentials (SSVEPs) from volunteers. They have much higher contact impedance present compared to Silver/Silver-Chloride coated electrodes, resulting in higher contact noise and more susceptibility to motion artifacts, but offer a wide range of benefits for low cost personalized electroencephalography.

## 1. Introduction

Electroencephalography (EEG) records the electrical signals generated by the summed neuronal activities within the human brain by placing multiple electrodes on the scalp [1]. As a sensing modality it has high time resolution, low cost, good portability, and is non-invasive; and as a result EEG has been widely used as a brain monitoring tool for applications ranging from epilepsy diagnosis to Brain-Computer Interfaces (BCIs) [2]. Traditionally, and particularly in clinical settings, *wet* Silver/Silver-Chloride (Ag/AgCl) electrodes have been used in most EEG experiments and recordings. This is due to the low body contact impedance (below 5 kOhm) and high-quality signal capturing allowed by adding a conductive gel between the electrode and the scalp. Nevertheless, wet EEG systems are difficult to set up, as they require a time-consuming skin preparation process and the conductive gel to be added. The electrodes are usually fabricated as circular disc or cup shapes.

More recently, *dry* EEG electrodes have become available commercially. Dry EEG electrodes are generally easier and quicker to setup because they require neither skin preparation nor a conductive gel. They can thus be more socially discrete, and have been investigated in clinical and home-based applications [3]. Dry electrodes have a high and

unstable contact impedance, which results in more noisy signal acquisition [4], but acceptable sensing performance can be obtained, particularly when using high input impedance EEG amplifiers [5]. Moreover, dry EEG electrodes may benefit from prolonged EEG recordings, as the sweat excreted from the scalp can moisturize the local area which lowers the contact impedance and improves the signal quality [6]. Systematic reviews of the state-of-the-art in dry EEG electrodes are available in [6, 7, 8, 9, 10]. From these we know that dry EEG electrodes can be made using various materials from metals, conductive polymers, and carbon, and can be made into different shapes such as finger-like, flat, micro-needles and other irregular shapes. Finger-like electrodes are the frequently used approach for haired regions on the head, as the fingers are able to penetrate through hair to contact with the scalp. Physical flexibility, allowing the fingers to deform under pressure, can help provide reasonable wearing comfort and scalp contact area.

Simultaneous to the need for dry EEG electrodes, there is an increasing awareness of the need for *inclusive* EEG, recognizing that a small number of sizes and shapes of electrode may not be the most appropriate for all different head shapes, types of hair, and electrical properties of skin [11]. There is thus a requirement to provide electrodes which can be personalized, while being physically flexible, and while allowing EEG to be recorded without the use of a conductive gel. In recent years 3D-printing of electrodes has been proposed as an approach which can provide electrodes meeting these criteria [12]. For example, [13] 3D-printed a clip-like electrode optimized for curly and coarse hair, especially for people of African descent. 3D-printing has been used for

\*Corresponding author

 le.xing@postgrad.manchester.ac.uk (L. Xing)

<https://www.research.manchester.ac.uk/portal/le.xing-postgrad.html> (L. Xing)

ORCID(s): 0000-0002-2507-6314 (L. Xing)

fabricating rigid fingered electrodes [14], flexible fingered electrodes [15], adjustable fingered electrodes with coiled springs for controlling pressure against the head [16], and concentric flat electrodes for real time noise cancellation [17]. However, these electrodes are all formed by printing a non-conductive base, which is then coated with a suitable conductive coating, typically Ag/AgCl as used in conventional electrodes, for signal monitoring. This coating process substantially increases the cost and manufacturing time.

This paper presents new 3D-printed EEG electrodes which are directly conductive, and so do not require coating in Ag/AgCl in order to measure the EEG. They are manufactured using a commercially available filament to decrease cost, and are both physically flexible and can operate without requiring a conductive gel. (We do not investigate it in this paper, but if desired both Ag/AgCl coatings and a conductive gel could be added to the new directly conductive electrodes here to improve performance, at the cost of time and price point.) Our new electrodes can be manufactured within 25–30 minutes, which we show to be faster and more cost-effective than existing 3D-printed electrodes. The new electrodes have a much higher contact impedance than Ag/AgCl coated dry electrodes, making them more susceptible to motion artifacts, but we show they can be used for the detection of Steady State Visual Evoked Potentials (SSVEPs). While [18] gave a brief blog post on the potential for printing directly conductive electrodes, the printed quality was very low. To our knowledge, this paper is the first systematic investigation into factors such as contact impedance, noise, and similar for directly conductive electrodes. A preliminary version of this work was presented in [19] as a conference paper. Here we substantially extend this work by considering a number of different electrode designs in terms of different shapes, finger lengths, and electrode-skin contact areas to demonstrate personalization, more extensive impedance and mechanical property measurements, and performing scanning electron microscopy to demonstrate the printed quality and to quantify the manufacturing benefits compared to previous approaches.

## 2. Materials and methods

### 2.1. Electrode design and manufacturing

A wide range of different EEG electrode designs and configurations have been created for 3D-printing [12]. In this work, we investigated both flat and finger-like electrodes, for non-haired and hairy parts of the head respectively. We considered the electrode shape, finger length, and skin contact area as different degrees of freedom in the design. As shown in Figure 1, we designed the electrodes into 3 basic categories: flat circle, short, and long fingered electrodes, with finger lengths of 7 mm (short) and 12 mm (long), respectively; each with 6 fingers. Each category contains 3 different skin contact areas at approximately: 110 mm<sup>2</sup> (small), 140 mm<sup>2</sup> (medium), 170 mm<sup>2</sup> (large), so that 9 types of directly conductive electrode were designed and made in total. All electrodes have a standard 4 mm snap

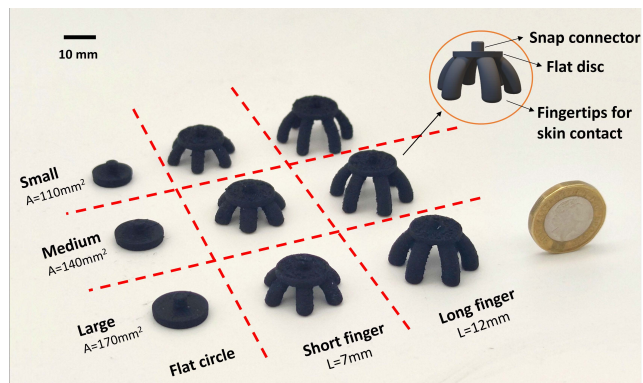


**Figure 1:** Different electrode designs in 3 categories: Flat circle, Short fingered (finger length 7 mm), and Long fingered (finger length 12 mm). Each category contains 3 different contact areas at 110 mm<sup>2</sup> ('Small'), 140 mm<sup>2</sup> ('Medium') and 170 mm<sup>2</sup> ('Large'), respectively. A UK £1 coin is included for scale.

connector printed on top so that they can be easily connected to most of state-of-the-art EEG amplifiers. Our electrode models are publicly available under an open source license at: <https://doi.org/10.48420/19148987>.

In general, the flat electrodes have a good contact quality with skin and thus are preferably used for non-hairy regions, whereas fingered electrodes have the potential to penetrate through the hair and are preferred for hairy regions. Compared to our previous flexible fingered Ag/AgCl coated electrodes (the flexible *Spider* type with 6 fingers in [15]), the new electrodes in this paper have been re-designed for the directly conductive filament used here to improve manufacturability. They feature wider finger contact points to the base for mechanical strength, and larger contact areas that enable the electrodes to have a more robust contact with scalp ensuring a better signal quality and lower electrode noise according to [20].

We used a desktop-grade 3D-printer (Lulzbot Mini) and a commercially available 3D-printing filament EEL (NinjaTek Inc, USA) which is made of Thermoplastic Polyurethane (TPU), providing flexibility, and carbon black, providing conductivity. The filament has an A90 shore hardness. Before use, we carefully examined the filament safety datasheet which indicates there are no known risks for skin contact. In terms of the manufacturing time, an individual flat circle electrode can be made within 10 minutes on average, and an individual fingered electrode (short and long finger) consumes about 25–30 minutes. After printing, the supporting structures and residuals can be easily removed for immediate use.

For a fair comparison, we also re-made the 3D-printed, Ag/AgCl coated, flexible electrodes from [15]. These followed the previous approach in [15], with a non-conductive base printed and then coated with Ag/AgCl ink (mixture 126-49 from Creative Materials Inc). However, we used the updated electrode shape designs made for this work, so that

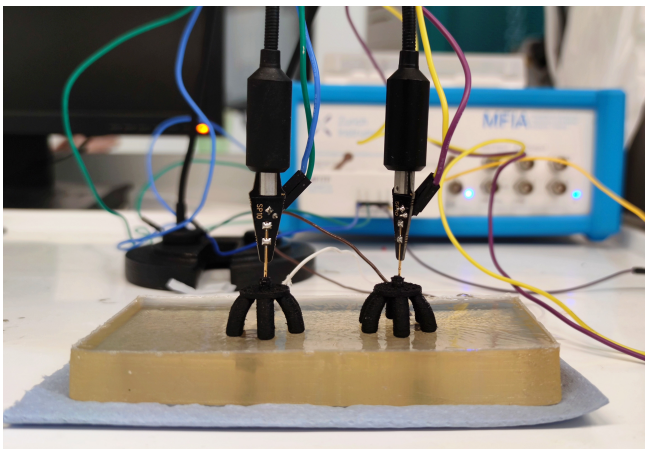


**Figure 2:** Contact impedance measurement setup on a small gelatine phantom. Two electrodes were placed on the phantom and connected with two probes.

the physical shapes for the electrodes were the same. Here we used the 6 finger version, with a ‘Medium’ contact area.

## 2.2. Electrical performance characterization

### 2.2.1. EEG phantom

To systematically characterize the electrical properties of the new electrodes, an EEG phantom was used for measurements of electrode contact impedance, contact noise, drift rate, and power line noise susceptibility. A cuboid phantom was used in this work, made of water and pork gelatine powder, as previously reported in [14, 21, 22]. Here we used 20% gelatine concentration per mass, with no added NaCl. The use of the gelatine phantom allows controllable and repeatable testing results compared to testing the electrodes on a person. On-person tests are used only for functional characterization, demonstrating typical signals collected (detailed in Section 2.4). All analyses described in this work were implemented in MATLAB 2021b (The MathWorks, Inc, US).

### 2.2.2. Contact impedance

The impedance during EEG recording plays a substantial role in accurate signal acquisition. High electrode contact impedance may increase the measurement’s susceptibility to various noise sources, resulting in a noisy signal collection. We investigated the contact impedance of electrodes against different frequencies ranging from 1 to 1000 Hz with an impedance analyzer (Zurich Instruments, Zurich, Switzerland). The setup of the contact impedance measurement on a gelatine phantom is shown in Figure 2.

In this setup, the measured total impedance consists of a double electrode contact impedance and the phantom impedance, with the latter assumed to be a constant factor in all tests allowing comparisons to be made. A similar setup was summarized in [23] for bioelectrical impedance measurements. Five samples for each electrode type were tested and then the average values and standard deviations were calculated.

### 2.2.3. Contact noise and drift

EEG recordings contain low level noise which may be caused by a number of sources, including the electronics of the EEG amplifier, the electrode-skin contact, and the electrode itself [20]. Therefore, measuring the signal collected from the phantom, which would be zero in the ideal case, provides insights into the electrode noise performance, as well as the drift rate/signal stability, and the susceptibility to power line noise. In this work, for all 10 electrode types (our 9 and the Ag/AgCl comparator), 5 electrode samples were tested and each sample was measured for 5 minutes. During the test, 2 electrodes were put onto a fresh phantom (similar to Figure 2) and the snap connectors were connected to a portable ActiWave EEG amplifier (CamNtech, Cambridge UK) with a sampling rate of 512 Hz to record the residual noise collected. Electronic noise from the EEG amplifier will be present in all of the recordings, and the amplitude of this is assumed to be a constant factor in all tests allowing comparisons to be made.

The recordings were pre-processed by deleting the approximately 30 s at the beginning of recordings to allow the setup to stabilize. Then, the low frequency contact noise, drift rate and the susceptibility to power line noise were determined by [14]:

- Contact noise: The raw data were bandpass filtered between 1 and 40 Hz with a 4<sup>th</sup> order Butterworth filter, and the recordings were split into 10 s segments. The Root-Mean-Square (RMS) of the signal was calculated for each segment as the contact noise.
- Drift rate: The raw recordings were low-pass filtered with the cut-off frequency at 0.16 Hz to extract the low-frequency signal changes, and then split into 30 s segments. The signal change or slope of each segment was calculated as the drift rate.
- Power line noise: The power line noise at 50 Hz was calculated by splitting the recordings into 10 s segments, followed by taking the Fast Fourier Transform (FFT) for each segment. The normalized single-side amplitude around 50 Hz was extracted to give the estimated power line noise pick-up amplitude.

## 2.3. Mechanical performance characterization

For dry EEG electrodes it is important to have a good physical contact with the head, which can be achieved by pushing the electrodes in more forcefully, at the obvious cost of user comfort (particularly for fingered designs). Mechanical performance is therefore a trade-off between manufacturing robustness, physical flexibility, contact impedance, and user comfort. To test the mechanical strength and flexibility of the fingered electrodes, a self-made 3D-printed lever and weights system was used. We gradually increased the applied force on the electrode, and at the same time captured a series of pictures to observe the changes in finger bending against the increased force. Using the comfortable pressure ranges for EEG electrodes pressing against the head as

demonstrated in [24], for an A90 shore hardness material, the maximum contact pressure was estimated at approximately 0.9 kg/cm<sup>2</sup> for the multi-finger dry EEG electrodes. Based on this, we estimated the maximum comfortable force when our electrodes are pushed against to the head should be approximately 5–6 N. We found Above 6 N, we increased the weights applied until the fingers fully collapsed, typically in the 20–30 N range (so well above the comfortable wearing range).

## 2.4. EEG sensing performance

### 2.4.1. On-phantom simulated signal recording

We also used the EEG phantom to investigate whether the new electrodes could accurately capture a pre-recorded signal *played-out* from the gelatine phantom. Compared to on-person tests, this gives a known signal to collect which can be directly compared against. The phantom for this purpose has two sintered Ag/AgCl electrodes embedded inside it during the making processing. (Note these are not shown in Figure 1 as for impedance tests no signal is played out.)

A pre-recorded EEG signal was streamed into the phantom via data acquisition equipment (NI USB-6363 X-series multi-function DAQ, National Instrument Inc, UK) and a Bi-Phasic Stimulus Isolator (DS4 Digitimer, UK). The input EEG signal was sampled at 1024 Hz and recorded from a volunteer who kept their eyes open for the first 30 s and eyes closed for the following 30 s. O2 (occipital, for recording) and A2 (mastoid, for reference) channels were used here for obtaining the EEG signal. This allows alpha (8–12 Hz) activity to be seen in the trace when the participant closed their eyes. The EEG collection was done in our lab with ethical approval by the University of Manchester Research Ethics Committee, application no. 2018-4015-5913. Participants gave written informed consent before taking part.

To record EEG played-out from the phantom, two electrodes were placed on the top of the phantom and connected to the ActiWave EEG amplifier with 1024 Hz sampling frequency. The measurement procedure was repeated for the 10 different electrode types. After obtaining these recordings, a highpass filter was applied to remove the DC offset and low frequency artifacts. Then, time-frequency analyses were implemented on both input and recorded signals by downsampling to 256 Hz and applying the ‘Morlet’-based Continuous Wavelet Transform (CWT). Here, we used the `image` function in MATLAB to generate a series of scalograms, which have a uniform color and magnitude scale for all plots for fair comparison. To quantify the similarities between the input EEG signal and different recordings of it, considering both the time and frequency domains, the normalized 2D cross-correlation (`norm2corr` function in MATLAB) was calculated between time-frequency images [25]. The maximum value was extracted for each electrode to give a representative similarity value.

### 2.4.2. On-person SSVEP monitoring

To test the sensing performance of our new electrodes, we performed a commonly used Steady-State Visual Evoked

Potential (SSVEP) experiment with volunteers. For compactness here we only tested the fingered electrodes, placed on haired regions of the head.

During the experiment, two electrodes were placed at EEG locations O2 (occipital) and A2 (mastoid) underneath an EEG cap, with an appropriate pressure applied to have a robust contact. These electrodes were connected to the ActiWave EEG amplifier with sampling frequency 1024 Hz. Visual flicking stimuli were generated at 7 Hz by using our smartphone Android App reported in [26]. Participants were asked to look at the smartphone screen flashing during the EEG recording, which is expected to produce a stimulus matched frequency peak in user’s EEG.

For each EEG recording, we extracted a 30 s clean EEG epoch, and applied a 50 Hz notch filter to remove power line noise and a high-pass filter to remove DC offset. Afterwards, the EEG power spectral density was calculated by applying a Welch transform with 1 s epoch, a Hamming window, 10% window overlap, and 2<sup>15</sup> FFT points. All on-person experiments were approved by the University of Manchester Research Ethics Committee, application no. 2018-4015-5913, and participants gave written informed consent before taking part.

## 2.5. Manufacturing performance characterization

To evaluate the printing quality of the electrodes, allowing us to quantify the costs involved, and to further investigate the mechanical properties of the electrodes, a Scanning Electron Microscope (SEM) was used to observe the cross-section of electrode fingers for both the Ag/AgCl coated and directly conductive electrodes. Fingers were cut in half, facing along the finger, and the cross-section coated with gold nanoparticles to increase its conductivity for better imaging quality.

## 3. Results and Discussion

### 3.1. Contact impedance

Figure 3 shows the contact impedance measured from the different electrode configurations. The contact impedance of our directly conductive electrodes is approximately 100 times higher than the previous Ag/AgCl coated 3D printed electrodes used here as a comparison. The contact impedance is also higher than other 3D-printed dry EEG electrodes summarized in [12]. As expected from [5], the electrodes with a larger contact area have lower contact impedance (large (blue) > medium (green) > small (orange)).

Despite a high contact impedance, the directly conductive electrodes should be able to obtain EEG signals. Focusing on 30 Hz as a standard frequency to measure at when attaching electrodes to a person, the new electrodes have impedance between 100–200 kΩ. [24] suggests that impedances below 250 kΩ should be sufficient for the state-of-the-art EEG amplifiers to collect a signal. Further, little pressure is used when holding the electrodes against the phantom (Figure 2). The contact impedance is expected to decrease if more pressure is applied [14, 24]. Higher contact

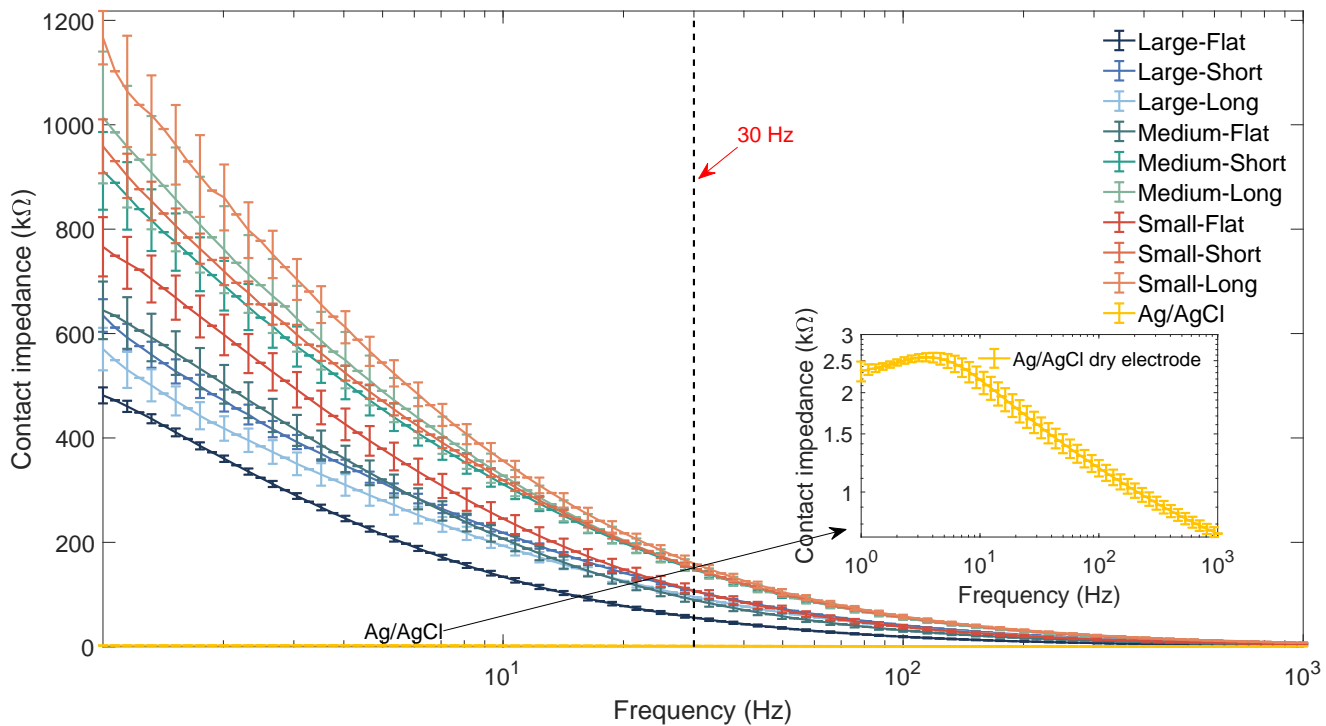


**Figure 3:** Contact impedance for all 10 electrode types with the frequency ranging from 1 to 1000 Hz. The contact area based groups were categorized as colors: Blue (Large), Green (Medium) and Orange (Small), as well as Yellow (Ag/AgCl comparison electrode). The contact impedance at 30 Hz is highlighted as a standard frequency to measure at when attaching electrodes on-person. Values range between 100–200 k $\Omega$  for the directly conductive electrodes.

impedance will make the system more sensitive to motion artifacts and similar interference sources as imbalances in electrode impedance are likely to be larger. Minimization of motion and the use of high input impedance amplifiers will thus be important for use of the directly conductive electrodes.

### 3.2. Contact noise and drift

Figure 4.A shows the Root-Mean-Squared noise between 1 and 40 Hz from the 10 electrodes being tested. Compared to the Ag/AgCl coated dry electrodes at below 1  $\mu$ Vrms, the directly conductive electrodes have more contact noise, with the average amplitude between 1–4  $\mu$ Vrms. Clean EEG normally has a amplitude ranging from approximately 10 to 100  $\mu$ V [27], so the contact noise with the novel electrodes will contaminate the EEG signal, but the noise level might be acceptable in many applications. Also, it is important to note that for each contact area group, the flat electrodes have the lowest levels of noise generation, most likely due to the shorter signal pathway present.

Figure 4.B shows the drift rate, and all electrodes have very low drift of below  $\pm 0.2 \mu$ V/min on average. This indicates that the electrodes can provide a stable EEG recording, and may be suitable for EEG monitoring during a long period of time. We do not find a clear relationship between the drift rate and electrode finger length or contact area.

Normally, power line noise will have only a small effect on EEG recordings as it can be readily filtered out, unless it leads to saturation to the amplifier which prevents the

underlying EEG signal from being collected. Figure 4.C shows the 50 Hz power line noise picked-up by all electrodes when connected to the phantom. Interestingly, regardless of different contact areas, the fingered electrodes are more sensitive 50 Hz interference than flat electrodes. Despite relatively high variance for the medium flat electrodes, the large, medium and small flat electrodes all have a very close performance to the Ag/AgCl coated electrode at around or below 1  $\mu$ V. The increased power line noise in fingered electrodes is possibly caused by the larger surface area exposed to the air, combined with the high impedance of the base material. Similar to the low frequency contact noise, 0–6  $\mu$ V power line noise will contaminate collected EEG signals, but noise at 50 Hz (or 60 Hz) is normally beyond the EEG frequencies of interest and can be effectively removed by applying digital notch filters. Nevertheless, an electrically shielded Faraday cage room, as used in many EEG experiments, would probably be beneficial to reduce interference.

### 3.3. Mechanical performance

Figure 5 shows an example of our mechanical testing, applying loads to flex the electrodes, here using the small-short fingered electrode. 6 N is estimated to be a suitable force that could maintain a stable contact as well as keep the user feeling comfortable for this electrode type, based on the comfortable pressure ranges reported in [24]. The vertical angle measured between the electrode finger and the center disc increased from 30.7° (no load) to 34.3° under 6 N (see Figure 5.A,B). When the applied force was

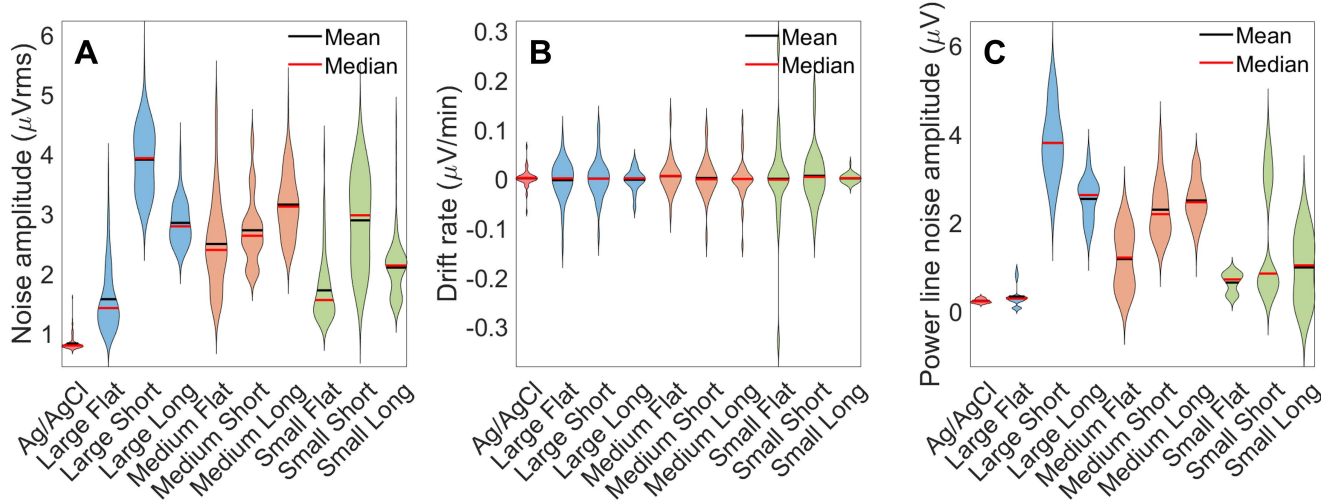


**Figure 4:** Violin plots of contact noise for all 10 electrode types. Red, blue, orange and green represent Ag/AgCl coated electrode, large, medium, and small directly conductive electrode categories respectively. (A) Root-Mean-Squared (RMS) contact noise between 1 and 40 Hz. (B) Drift rate. (C) 50 Hz power line noise pick-up.

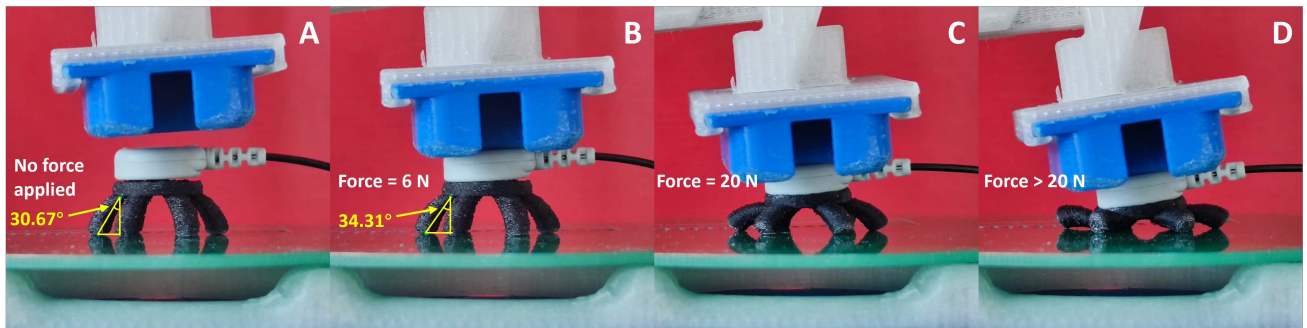


**Figure 5:** Example of the mechanical performance test on a small short fingered electrode. (A) Without load, the vertical angle between the flat base and the finger is  $30.7^\circ$ . (B) Under a comfortable force of 6 N the angle increases to  $34.3^\circ$ . (C) Under 20 N the electrode fingers are fully compressed. (D) The electrode fingers are irreversibly broken at an over-deforming force.

increased gradually, the finger was deformed further and fully compressed after applying approximately 20 N (see Figure 5.C,D). Complete collapse resulted in irreversible fractures forming, but the force threshold for finger breaking is far away from the comfortable force range.

For the electrodes with larger contact areas, the comfortable force is expected to be bigger than 6 N. Nevertheless, 6 N was still considered as a suitable value to use for testing all electrode configurations. The finger angle bending change, and the breakage force threshold range, are given in Table 1. The finger angle change under 6 N is very small for all electrode types, causing no damage to electrodes under a comfortable force, making them suitable for on-person EEG monitoring with some flexibility for fitting and comfort. Importantly, at the same contact area, short fingered electrodes are able to bear larger force than long fingered electrodes, showing better mechanical strength but with a worse mechanical flexibility. Similarly, at the same finger length, the finger breaking threshold range for electrodes with larger contact area is much higher than smaller electrodes. For example, the ‘Large-Short’ configuration can

support over 50 N of force, showing better mechanical strength but sacrificing flexibility. Therefore, considering the trade-off between mechanical strength and flexibility, the electrode with a medium strong and long fingers could probably satisfy both requirements in this case, suggesting some clear directions for the future 3D-printed and customized electrodes design.

### 3.4. On-phantom simulated signal recording

Figure 6.A and L show the time-frequency scalogram and power spectrum density, respectively, of the pre-recorded EEG used with the phantom. These show the *ideal* signal which would be re-recorded exactly by the new electrodes if no noise or other factors were present. As shown clearly, during the period of eyes closed (30–60 s), alpha activity at around 10 Hz becomes dominant, highlighted as a red squared block in Figure 6.A and red peak in Figure 6.L. Figures 6.B–K show the scalograms of the signals recorded from the large (Figure 6.B–D), medium (Figure 6.E–G), small (Figure 6.H–J), and Ag/AgCl coated (Figure 6.K) electrodes when connected to the EEG phantom. All of the

**Table 1**

Electrode finger bending changes and finger-breaking thresholds

Electrode type	Small Short		Small Long		Medium Short		Medium Long		Large Short		Large Long	
	Without	With	Without	With	Without	With	Without	With	Without	With	Without	With
Deforming angle (without/with 6 N)	30.7°	34.3°	28.4°	32.0°	34.3°	37.5°	27.6°	30.8°	32.0°	34.9°	25.4°	27.8°
Angle change under 6 N	3.6°		3.6°		3.2°		3.2°		2.9°		2.4°	
Finger breaking threshold	16–20 N		16–20 N		30–35 N		22–26 N		50–60 N		30–35 N	

**Table 2**

Time-frequency scalogram similarities between input EEG and different recordings

Electrode type	Normalized 2D cross-correlation
Large-Flat	0.93
Large-Short	0.84
Large-Large	0.94
Medium-Flat	0.96
Medium-Short	0.89
Medium-Long	0.88
Small-Flat	0.87
Small-Short	0.89
Small-Long	0.85
Ag/AgCl coated	0.96

electrodes clearly capture the alpha activity burst during 30–60 s, despite some low frequency noise present in some of scalograms, as would be predicted from the noise analysis in Section 3.2.

To quantify the quality of data collected from the new electrodes, Table 2 shows the maximum cross correlation value for each scalogram when compared with the *template*—that is, the scalogram of the pre-recorded EEG in Figure 6.A. In general, the signals from directly conductive electrodes (between 0.84–0.96) are slightly less than the Ag/AgCl electrode (at 0.96), but very close, particularly for the ‘Large-Large’ electrode configuration. This is what can be expected, as the conductive material naturally leads to more noise in the signal collection, which can be decreased with larger electrodes. However, the increased noise may not be a substantial problem in some EEG applications, as it can be rejected via digital signal processing steps. Notably, this phantom testing system provides a controlled, repeatable, and systematic method for evaluating the sensing performance of different electrodes, which could possibly be standardized for novel EEG electrode testing in other research.

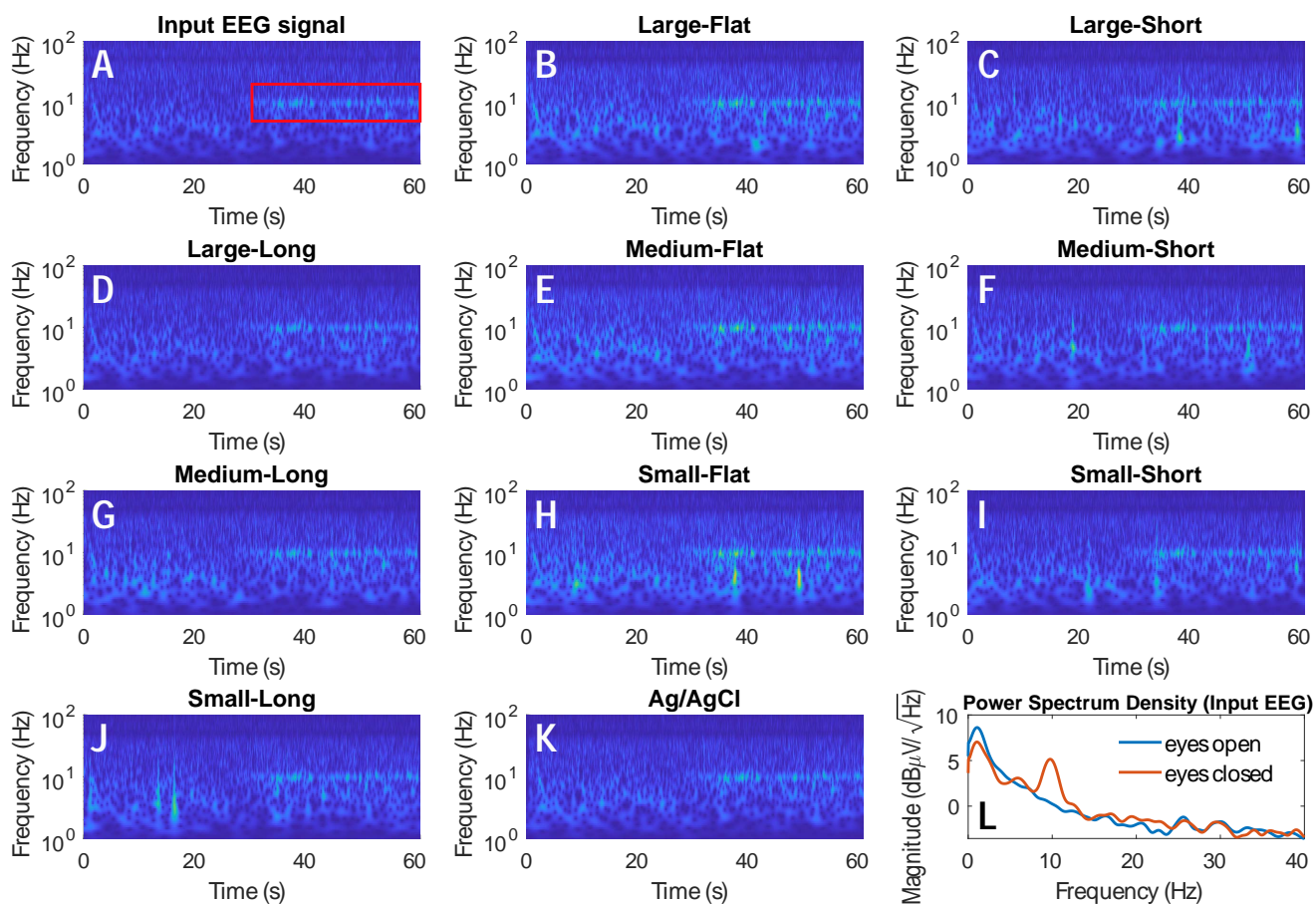
### 3.5. On-person SSVEP monitoring

Figure 7 shows examples of the SSVEP detected by different fingered electrodes in the frequency domain when using 7 Hz visual stimulation with a volunteer participant. The induced SSVEPs show a clear peak at the stimulation

frequency compared to the baseline case with no stimulation present. Moreover, the first harmonic at 14 Hz can also be seen for some of the electrodes, as expected from [28]. Defining Signal-to-Noise Ratio (SNR) as the difference between the baseline and SSVEP peak at the stimulation frequency, the directly conductive electrodes can obtain an SNR between 5.8 dB and 10.3 dB, whereas the Ag/AgCl coated electrode has a SNR of around 7 dB. The SNR of conductive electrodes varies, but all show a good detectability of SSVEPs, even outperforming the Ag/AgCl in some cases. As power spectral density is calculated via the Welch transform, multiple epochs of data are averaged together, reducing the effect of random electrode noise which tends to average to zero, allowing this good performance, assuming the data collection time is acceptable. Here, the Ag/AgCl coated electrode was expected to be better for on-person EEG monitoring due to its low impedance, but it does not outperform all directly conductive electrodes, which is reasonably caused by the minor variance of electrode contact quality, minor variance of electrode position, and minor changes in the person between recordings.

### 3.6. Manufacturing performance

To investigate the manufacturing performance, Figure 8 shows SEM cross sections of example electrode fingers. Figure 8.A shows a finger from our previous 3D-printed flexible Ag/AgCl coated electrode. Made of pure Thermoplastic polyurethane (TPU) it has a better printing quality



**Figure 6:** Time-frequency analysis of the signals tested on a gelatine phantom, the scalograms were obtained by using Morlet based continuous wavelet transform. (A) Pre-recorded EEG signal played-out from the phantom, with alpha oscillation during 30–60 s highlighted by a red rectangle. Signals recorded by using 'Large'(B–D), 'Medium'(E–G), and 'Small'(H–J) directly conductive electrodes, and an Ag/AgCl coated dry electrode for comparison (K). (L) Power spectral density of the input EEG signal, with a clear 10 Hz peak present during eyes closed.

with a very good compactness in the cross-section view. The Ag/AgCl coating layer can be readily seen and its thickness is highlighted. In contrast, Figure 8.B displays a finger cross-section from one of the new directly conductive electrodes. It shows a large number of hollows inside the electrode finger, as well as a rough printing surface, which probably explains the non-ideal mechanical strength of this printing filament that was a mixture of TPU and carbon black. It is possible, and likely, that future conductive flexible filaments will allow an improved printing quality which may lead to better quality electrodes.

Based upon the SEM images, we estimated and compared the manufacturing costs for both 3D-printed fingered Ag/AgCl coated electrodes and directly conductive electrodes. The 3D-printed Ag/AgCl coated electrodes require a series of manufacturing procedures: first printing the non-conductive base structure; then conductive coating with Ag/AgCl; and lastly curing the coating; which requires 40–60 minutes in our lab to make an individual fingered electrode. (Making multiple electrodes at the same time is potentially quicker as the coating and curing steps can be shared.) Based on Figure 8.A, the thickness of the Ag/AgCl

coating was measured at between 110–170  $\mu$ m. The total surface area of the Ag/AgCl electrode we used here was estimated at 1220 mm<sup>2</sup>. Based on this, if taking 150  $\mu$ m as the average coating thickness, we estimate that the volume of cured Ag/AgCl ink required for one electrode is 0.2 cm<sup>3</sup>. Considering that the Ag/AgCl ink density is 3.39 g/mL and pure silver has density of 10.49 g/cm<sup>3</sup>, we estimate the Ag/AgCl ink required for one electrode is about 1 mL, allowing for a small amount of ink waste during the dip coating process. At 2021 prices for the used Ag/AgCl ink, the coating alone consumes £4–5 per electrode. Also, the printing filament required costs approximately £0.3 per electrode, and the curing processing required after coating costs extra electricity. (Here we ignore the capital costs of the 3D-printer and oven.) Therefore, the complete manufacturing cost of an Ag/AgCl coated electrode consists of printing, filament, Ag/AgCl coating inks (including waste) and curing, which costs approximately £5 per electrode. Such high cost will significantly limit personalized EEG monitoring in the future consumer market.

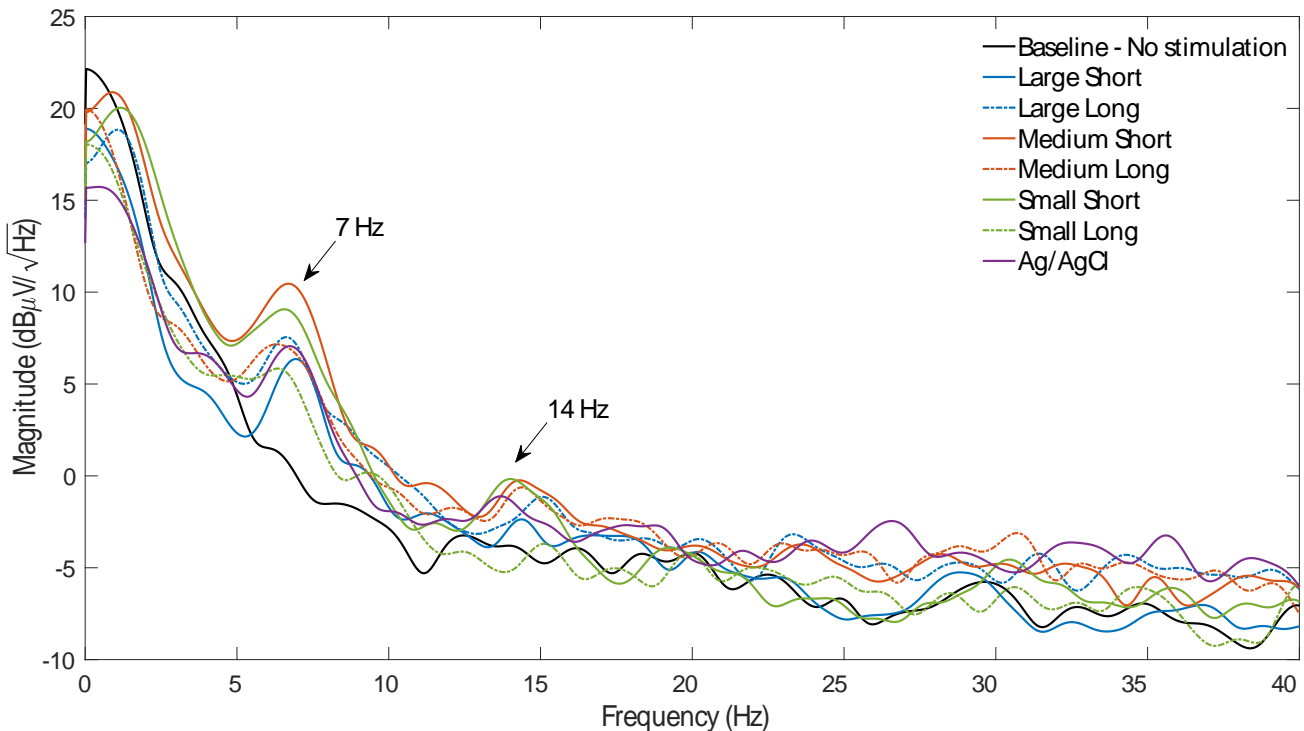


**Figure 7:** On-person detection of Steady-State Visual Evoked Potentials (SSVEP) with the stimulation frequency at 7 Hz, by using the fingered electrodes on the occipital lobe. The first harmonic occurs at 14 Hz.

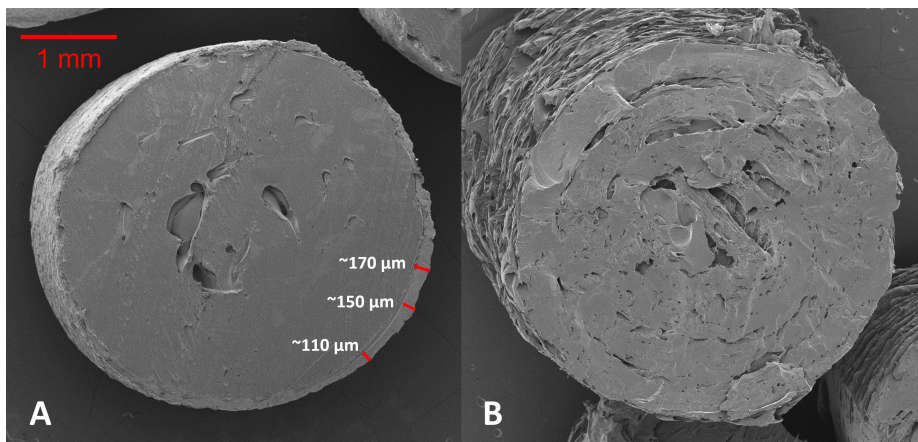


**Figure 8:** Cross-sections of electrode fingers under SEM. (A) Ag/AgCl coated dry electrode. (B) Directly conductive electrode.

In contrast, the directly conductive electrode only requires a printing process, consuming approximately 30 minutes and about £0.5 per electrode. The flat electrodes can be printed in a multiple number mode, with an average of 10 minutes consumed per electrode. The decreased manufacturing cost and time is substantially more credible for enabling personalized EEG monitoring. The cost of a commercial disposable Ag/AgCl EEG electrode varies for different suppliers, but a reasonable average in our experience is £1 per electrode, higher than our new electrodes and without the possibilities of personalized EEG monitoring. These manufacturing comparisons are summarized in Table 3.

#### 4. Conclusions

This paper has used 3D-printing and a commercially available filament to successfully demonstrate a low cost, directly conductive, physically flexible, dry EEG electrode. Compared to previous 3D-printed EEG electrodes our electrodes do not require an Ag/AgCl conductive coating to be used. Rapid manufacturing, low cost, and potential for personalization enables our electrodes to be used in next generation wearable EEG systems and BCI applications. We demonstrated that these novel electrodes can collect EEG for the detection of Steady-State Visual Evoked Potentials (SSVEPs). Although the electrode-skin contact impedance

**Table 3**

Manufacturing cost estimation for Ag/AgCl coated and directly conductive 3D-printed electrodes, per electrode, assuming manufactured one at a time

Electrode type	Ag/AgCl coated 3D-printed	Directly conductive 3D-printed	Commercial disposable Ag/AgCl
Costs come from	Printing + Filament + Ag/AgCl ink + Curing	Printing + Filament	—
Manufacturing cost (£)	≈ 5.0	≈ 0.5	≈ 1.0
Manufacturing time (minutes)	≈ 40–60 (Printing + Coating + Curing)	≈ 30 (Printing only)	—
Personalization ability	✓	✓	✗

is higher than Ag/AgCl coated dry electrodes, leading to increased sensitivity to various artifacts, the electrodes are still capable of capturing an EEG signal with compatible EEG amplifiers. We do not investigate it in this paper, but if desired both Ag/AgCl coatings and a conductive gel could be added to the new directly conductive electrodes to improve performance, at the cost of time and price point. Future work may need to focus on developing novel 3D-printed EEG headsets that could fit in with these novel electrodes to provide a more robust electrode contact with scalp, which is also an open challenge in this research field. Lastly, this work provides some directions for manufacturers to optimize their formulation of the directly conductive material to improve its electrical and mechanical properties for better applications.

## 5. Acknowledgment

The authors would like to thank Huize Luo for her technical support during the SEM imaging, and also thank Liam Johnson and Dr. Chao Wu for their technical support for the electrode-phantom contact impedance setup.

## CRediT authorship contribution statement

**Le Xing:** Conceptualization, electrode modeling, manufacturing and testing, data analysis, paper writing. **Alexander J. Casson:** Conceptualization, data analysis, paper editing, supervision.

## References

- [1] A. J. Casson, M. Abdulaal, M. Dulabh, S. Kohli, S. Krachunov, E. Trimble, *Electroencephalogram*, in: *Seamless Healthcare Monitoring*, Springer, 2018, pp. 45–81.
- [2] A. J. Casson, Wearable EEG and beyond, *Biomedical engineering letters* 9 (2019) 53–71.
- [3] H. Hinrichs, M. Scholz, A. K. Baum, J. W. Kam, R. T. Knight, H.-J. Heinze, Comparison between a wireless dry electrode EEG system with a conventional wired wet electrode EEG system for clinical applications, *Scientific reports* 10 (2020) 1–14.
- [4] G. Li, S. Wang, Y. Y. Duan, Towards gel-free electrodes: A systematic study of electrode-skin impedance, *Sensors and Actuators B: Chemical* 241 (2017) 1244–1255.
- [5] E. H. T. Shad, M. Molinas, T. Ytterdal, Impedance and noise of passive and active dry EEG electrodes: a review, *IEEE Sensors Journal* 20 (2020) 14565–14577.
- [6] Y. M. Chi, T.-P. Jung, G. Cauwenberghs, Dry-contact and noncontact biopotential electrodes: Methodological review, *IEEE reviews in biomedical engineering* 3 (2010) 106–119.
- [7] M. A. Lopez-Gordo, D. Sanchez-Morillo, F. P. Valle, Dry EEG electrodes, *Sensors* 14 (2014) 12847–12870.
- [8] G. Di Flumeri, P. Aricò, G. Borghini, N. Sciaraffa, A. Di Florio, F. Babiloni, The dry revolution: evaluation of three different EEG dry electrode types in terms of signal spectral features, mental states classification and usability, *Sensors* 19 (2019) 1365.
- [9] Y. Fu, J. Zhao, Y. Dong, X. Wang, Dry electrodes for human bioelectrical signal monitoring, *Sensors* 20 (2020) 3651.
- [10] C. Im, J.-M. Seo, A review of electrodes for the electrical brain signal recording, *Biomedical Engineering Letters* 6 (2016) 104–112.
- [11] T. Choy, E. Baker, K. Stavropoulos, Systemic racism in EEG research: considerations and potential solutions, *Affective Science* 3 (2022) 14–20.
- [12] L. Xing, J. C. Batchelor, A. J. Casson, Opportunities and challenges for flexible and printable electrodes in electroencephalography, in: *2021 IEEE International Conference on Flexible and Printable Sensors and Systems (FLEPS)*, IEEE, 2021, pp. 1–4.
- [13] A. Etienne, T. Laroia, H. Weigle, A. Afelin, S. K. Kelly, A. Krishnan, P. Grover, Novel electrodes for reliable EEG recordings on coarse and curly hair, in: *2020 42nd Annual International Conference of the IEEE Engineering in Medicine & Biology Society (EMBC)*, IEEE, 2020, pp. 6151–6154.
- [14] S. Krachunov, A. J. Casson, 3D printed dry EEG electrodes, *Sensors* 16 (2016) 1635.
- [15] A. Velcescu, A. Lindley, C. Cursio, S. Krachunov, C. Beach, C. A. Brown, A. K. Jones, A. J. Casson, Flexible 3D-printed EEG electrodes, *Sensors* 19 (2019) 1650.
- [16] M. Kimura, S. Nakatani, S.-I. Nishida, D. Taketoshi, N. Araki, 3D printable dry EEG electrodes with coiled-spring prongs, *Sensors* 20 (2020) 4733.
- [17] H. Cowan, S. Daryanavard, B. Porr, R. Dahiya, A real-time noise cancelling EEG electrode employing deep learning, *arXiv preprint arXiv:2011.03466* (2020).
- [18] Conor Russomanno blog: 3D printed EEG electrodes, 3D printed EEG electrodes, 2016. URL: <https://conorrussomanno.com/2015/02/16/3d-printed-eeg-electrodes/>.
- [19] L. Xing, A. J. Casson, Directly conductive, flexible, 3D printed, EEG electrodes, in: *2022 IEEE International Conference on Flexible and Printable Sensors and Systems (FLEPS)*, IEEE, 2022, pp. 1–4.
- [20] E. Huigen, A. Peper, C. Grimbergen, Investigation into the origin of the noise of surface electrodes, *Medical and biological engineering and computing* 40 (2002) 332–338.
- [21] S. Kohli, A. J. Casson, Removal of gross artifacts of transcranial alternating current stimulation in simultaneous EEG monitoring, *Sensors* 19 (2019) 190.
- [22] A. Y. Owda, A. J. Casson, Investigating gelatine based head phantoms for electroencephalography compared to electrical and ex vivo porcine skin models, *IEEE Access* 9 (2021) 96722–96738.

- [23] T. K. Bera, Bioelectrical impedance methods for noninvasive health monitoring: a review, *Journal of medical engineering* 2014 (2014).
- [24] P. Fiedler, R. Mühle, S. Griebel, P. Pedrosa, C. Fonseca, F. Vaz, F. Zanow, J. Haueisen, Contact pressure and flexibility of multipin dry EEG electrodes, *IEEE transactions on neural systems and rehabilitation engineering* 26 (2018) 750–757.
- [25] J.-C. Yoo, T. H. Han, Fast normalized cross-correlation, *Circuits, systems and signal processing* 28 (2009) 819–843.
- [26] N. K. Jacob, H. O. Kings, A. J. Casson, A smartphone based platform for portable non-invasive light and sound neuromodulation, in: 2020 42nd Annual International Conference of the IEEE Engineering in Medicine & Biology Society (EMBC), IEEE, 2020, pp. 5228–5231.
- [27] I. Daly, F. Pichiorri, J. Faller, V. Kaiser, A. Kreilinger, R. Scherer, G. Müller-Putz, What does clean EEG look like?, in: 2012 Annual International Conference of the IEEE Engineering in Medicine and Biology Society, IEEE, 2012, pp. 3963–3966.
- [28] G. R. Müller-Putz, R. Scherer, C. Brauneis, G. Pfurtscheller, Steady-state visual evoked potential (SSVEP)-based communication: impact of harmonic frequency components, *Journal of neural engineering* 2 (2005) 123.

## 6. Biographies



**Le Xing** received the B.E. in Bioengineering and M.Sc. degree in Biomedical Engineering from Southeast University, China and the University of Bristol, UK, in 2018 and 2019, respectively. He is currently a PhD candidate at the University of Manchester, in the Department of Electrical and Electronic Engineering. His research interests include wearable EEG, printed EEG electrode development, EEG signal processing, and Brain-Computer Interfaces.



**Alex Casson** is currently a Reader (Associate Professor) in the Department of Electrical and Electronic Engineering at the University of Manchester; Visiting Reader in the School of Medicine at the University of Leeds; Honorary Reader in the Medical Physics Department at Northern Care Alliance NHS Foundation Trust; Fellow of the Alan Turing Institute; and Bioelectronics technology platform lead at the Henry Royce Institute. He gained his undergraduate degree from the University of Oxford in 2006, and completed his PhD from Imperial College London in 2010. His research includes non-invasive bioelectronics interfaces, wearables for human body monitoring, and sensor signal processing and machine learning.